Rotating Rayleigh-Taylor instability

M. M. Scase,[1,*] K. A. Baldwin,[2] and R. J. A. Hill[3]

[1]*School of Mathematical Sciences, University of Nottingham, Nottingham NG7 2RD, United Kingdom*
[2]*Faculty of Engineering, University of Nottingham, Nottingham NG7 2RD, United Kingdom*
[3]*School of Physics and Astronomy, University of Nottingham, Nottingham NG7 2RD, United Kingdom*

The effect of rotation upon the classical Rayleigh-Taylor instability is investigated. We consider a two-layer system with an axis of rotation that is perpendicular to the interface between the layers. In general, we find that a wave mode's growth rate may be reduced by rotation. We further show that in some cases, unstable axisymmetric wave modes may be stabilized by rotating the system above a critical rotation rate associated with the mode's wavelength, the Atwood number, and the flow's aspect ratio.

I. INTRODUCTION

Understanding of the Rayleigh-Taylor instability has increased progressively since Lord Rayleigh's [1] initial work and the investigations of Taylor [2] and Lewis [3]. The motivation for research into this fundamental problem has changed over time, from the original interests of Taylor and Lewis to the energy supply and astrophysical aspects of more recent work. The now familiar structure of the Rayleigh-Taylor instability has been observed from small scales in, for example, inertial confinement fusion problems (see, e.g., [4]) to extremely large scales, such as the crab nebula (see, e.g., [5]) where pulsar winds accelerate through dense supernova remnants. In many cases of practical interest, it would be desirable to have some further control over the instability after the setting of the initial density profiles. One possibility is to rotate the system; the often stabilizing effect of rotation on a flow is well known (see, e.g., [6]). Tao *et al.* [7] investigated whether rotation may be used to influence the Rayleigh-Taylor instability at the surface of an inertial confinement fusion target by considering instability at an interface *parallel* to the axis of rotation. In inertial confinement fusion, the Rayleigh-Taylor instability reduces the efficiency of fusion during both the acceleration phase, between the ablator and the fuel, and the deceleration phase, between the hot and cold fuel regions (see, e.g., [8]). The efficiency is reduced due to the increased interfacial surface area between the two layers in each case. The work of Tao *et al.* [7] suggested that the instability may be suppressed around the equatorial region of a spherical rotating target.

In a previous paper [9] we reported results of experiments to study the development of the Rayleigh-Taylor instability in a two-layer fluid system with axis of rotation perpendicular to the layers. The presence of rotation introduces a restoring force on fluid elements moving perpendicular to the axis of rotation: the Coriolis force. This fictitious force, which appears in a rotating reference frame, acts to restore a fluid element, traveling in a direction perpendicular to the axis of rotation, to its original position, following a curved path. The presence of the Coriolis force therefore allows the fluid to support inertial wave motions, the rotational counterpart to the internal gravity waves supported by a density stratification (see, e.g., [10,11]). As will be shown, the Coriolis force acts to inhibit large-scale overturning motions at the unstable interface and is consequently important in changing the character of the developing Rayleigh-Taylor instability as the rate of rotation is increased. The effect is shown qualitatively in Fig. 1. It can be seen that the large-scale overturning motion required to form large vortices (top) is restricted in the presence of rotation (bottom).
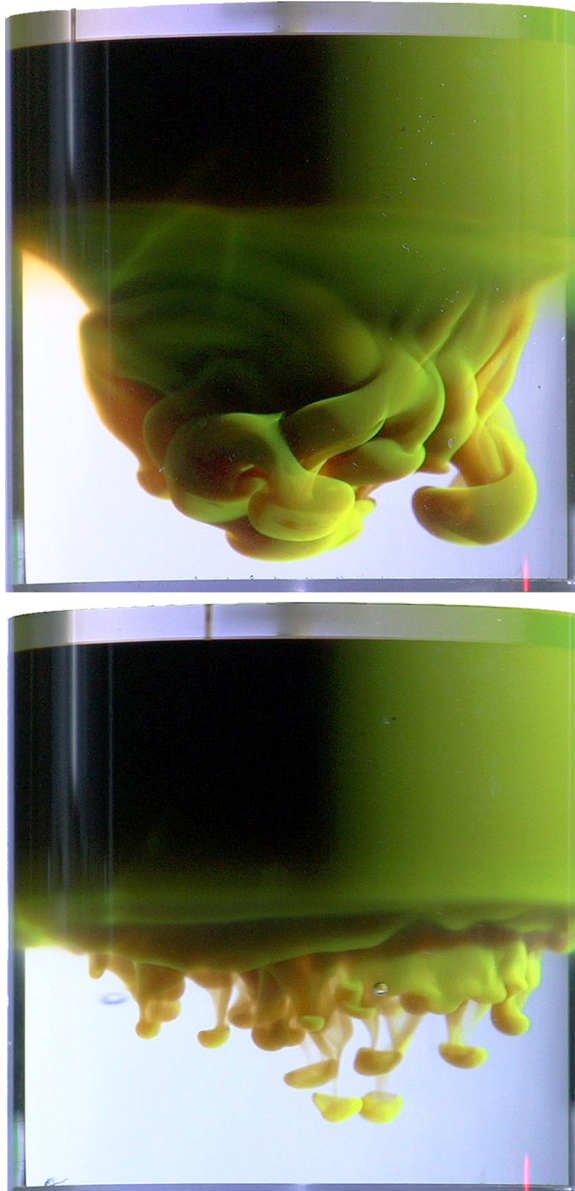
---

*matthew.scase@nottingham.ac.uk

FIG. 1. The top image, taken from our experiments (image layout modified from [12]), is of a magnetically induced Rayleigh-Taylor instability developing in a nonrotating system. The instability develops in time, forming large vortices that transport the green fluid downward. The bottom image is of the same fluids, but here the system is rotating. The effect of the rotation can be seen to restrict the size of the vortices that form and inhibit the bulk vertical transport of fluid. The times shown are 1.92 and 3.52 s after initiation in the top and bottom images, respectively. The experiments are described in Refs. [9,12]. The tank diameter is 90 mm and the rotation rate in the bottom image was 2.52 rad s^{-1}.

In this paper we present a theoretical study of the Rayleigh-Taylor instability under the influence of rotation. Miles [13,14] considered the effects of rotation on infinitesimal free-surface waves on a body of water, remarking on Fultz's [6] observation that the parabolic nature of the free-surface is important and cannot be neglected as previous authors had (see, e.g., [15]): "The planar [horizontal

hydrostatic interface] approximation is necessarily inconsistent for axisymmetric gravity waves in the sense that both the rotation induced shift... and the free-surface slope are of the same order of magnitude." We develop the theory of Miles [13,14] to allow for a two-layer fluid system that may have either a stable or an unstable interface. We find in the limit of high, stable density difference that we recover Miles' [14] result and in the limit of an unstable density difference with no rotation we recover the classical Rayleigh-Taylor model [2]. In the special limit of semi-infinite fluid layers and a strictly horizontal interface we recover the model of Chandrasekhar [16]. We develop the dispersion relation for perturbations to an interface between two fluid layers in the low-rotation-rate limit. For axisymmetric waves we are able to find a critical rotation rate above which a given wave mode behaves as an oscillating standing wave, but below which it exhibits Rayleigh-Taylor growth. In general, nonaxisymmetric waves cannot be stabilized indefinitely, but we are able to say for a given mode whether the growth rate is reduced or increased by rotation and find that there is a strong dependence on the aspect ratio of the layers.

In Sec. II we develop an inviscid theory based on the previous theories of Rayleigh-Taylor instability due to Taylor [2] and the modeling of surface oscillations on rotating bodies of fluid due to Lamb [15] and Miles [13,14]. The key results are a dispersion relation for axisymmetric and asymmetric perturbations to the interface of a rotating two-layer fluid system (both stable and Rayleigh-Taylor unstable), a critical rotation rate for stabilizing Rayleigh-Taylor unstable axisymmetric modes of perturbation. In Sec. III we discuss our results and draw our conclusions.

II. MODELING

A. Growth of the instability

We begin by considering a two-layer rotating fluid as shown in Fig. 2. The upper layer is denoted by a subscript 1 and the lower layer by a subscript 2. We assume cylindrical polar coordinates with unit vectors $\boldsymbol{e}_r$, $\boldsymbol{e}_\theta$, and $\boldsymbol{e}_z$ in the radial, azimuthal, and vertical directions, respectively, and take the rotation to be described by the pseudovector $\boldsymbol{\Omega} = \Omega \boldsymbol{e}_z$. The radius of the cylinder is a and the lid and base of the cylinder are at $z = \pm d$. The whole system may be accelerated vertically at a rate g_1. Ignoring the effects of viscosity, we write the rotating Euler equation for the fluid in each layer as

$$\frac{D\boldsymbol{u}_j}{Dt} = -\frac{1}{\rho_j}\boldsymbol{\nabla} p_j + \boldsymbol{g}^* - \boldsymbol{\Omega} \times (\boldsymbol{\Omega} \times \boldsymbol{x}) - 2\boldsymbol{\Omega} \times \boldsymbol{u}_j \tag{1}$$

for $j = 1,2$, where $\boldsymbol{g}^* = -(g + g_1)\boldsymbol{e}_z$ and $\boldsymbol{u}_j$ and $\boldsymbol{x}$ are velocity and position vectors, respectively, in the rotating frame. For simplicity, we drop the g_1 notation and will write $\boldsymbol{g}^* = -g\boldsymbol{e}_z$, with the understanding that g may not be equal to the acceleration due to gravity and may change sign as a result of external bulk acceleration of the system.

When the fluid system is spun up into a hydrostatic regime (in the rotating, noninertial reference frame) then $\boldsymbol{u}_j \equiv \boldsymbol{0}$ and

$$p_j = p_0 - \rho_j \left\{ gz - \frac{\Omega^2}{2}\left(r^2 - \frac{1}{2}a^2\right) \right\}, \quad j = 1,2, \tag{2}$$

where p_0 is a constant reference pressure equal to the pressure at the interface when the system is not rotating. We take $z = z_0(r)$ to be the position of the interface between the two fluid layers. In the absence of viscosity, requiring the stress to be continuous across the interface is equivalent to requiring continuity of pressure across the interface. Hence we may write $p_1 = p_2$ on $z = z_0(r)$ and it follows that the interface is an isobar on which $p_j = p_0$ and has a profile given by

$$z_0(r) = \frac{\Omega^2\left(r^2 - \frac{1}{2}a^2\right)}{2g}, \tag{3}$$

constrained by $\int_0^a z_0(r) r \, dr = 0$ to ensure that the fluid layers are of equal depth. The shape and position of the interface are independent of the densities of the fluid in the upper and lower layers. Hence, while the value of p_0 and the stability of the interface may change according to whether
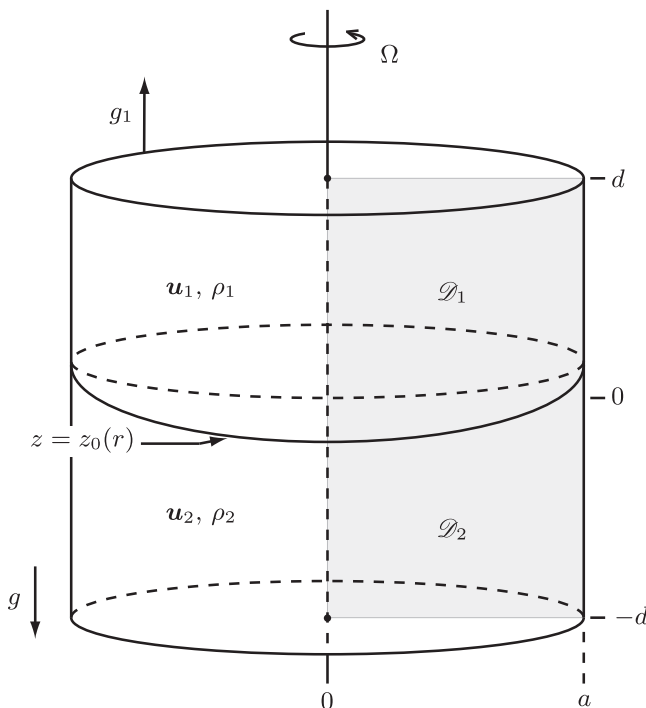
FIG. 2. Two layers of incompressible fluid of density ρ_1 and ρ_2 occupy a cylindrical tank of radius a that is being accelerated (see [2]) at a rate g_1. When the tank is not rotating we take the interface between the fluids to be at $z = 0$ (coordinates moving with the tank), the base of the tank at $z = -d$, and the lid of the tank at $z = d$. The tank is spun up to have a constant angular velocity Ω about the z axis. The isobar describing the interface is given by $z = z_0(r)$ where $z_0(r) = \Omega^2(r^2 - \frac{1}{2}a^2)/2g$ and $p = p_0$ on $z = z_0(r)$. The meridional plane is split into two domains $\mathscr{D}_1$ and $\mathscr{D}_2$ representing the upper and lower layers, respectively (shaded gray).

$\rho_1 < \rho_2$ or vice versa, the profile remains the familiar concave paraboloid such as may be observed at the free surface of a vigorously stirred beverage.

Following Taylor [2], we investigate the development of the Rayleigh-Taylor instability under rotation by considering the development of a perturbation to the interface. The strength of a stratification can be characterized by an Atwood number, defined here as $\mathscr{A} = (\rho_2 - \rho_1)/(\rho_2 + \rho_1)$. Using this definition, we have that for a stable stratification $\mathscr{A} > 0$ and for an unstable stratification $\mathscr{A} < 0$. (N.B. In experimental investigations of the Rayleigh-Taylor instability, many authors, dealing only with unstable flows, define the Atwood number with opposite sign.) The amplitude of the perturbation and the velocity and pressure deviation from the hydrostatic are all assumed to be small. We describe the fluid velocity and pressure perturbations in terms of a scalar potential, unifying the approaches of Taylor [2], in modeling the nonrotating Rayleigh-Taylor instability, and Miles [13,14], in modeling surface waves on a rotating fluid. Taylor [2] used a standard velocity potential and Miles [14] used an acceleration potential of the kind proposed by Poincaré [17]. Here we make use of the generalized potential described by Hart [18]. Specifically, for an interface perturbation

$$z = z_0(r) + \epsilon\zeta(r,\theta,t), \tag{4}$$

where $\epsilon|\zeta| \ll d$, we take the velocity perturbation to the hydrostatic background to be

$$\boldsymbol{u}_j = \epsilon\left\{\left(1 + \frac{1}{4\Omega^2}\frac{\partial^2}{\partial t^2}\right)\boldsymbol{\nabla}\phi_j - \frac{1}{2\Omega}\frac{\partial}{\partial t}(\boldsymbol{e}_z \times \boldsymbol{\nabla}\phi_j) + \boldsymbol{e}_z \times (\boldsymbol{e}_z \times \boldsymbol{\nabla}\phi_j)\right\} \tag{5}$$

for $j = 1,2$ and the pressure to be

$$p_j = p_0 - \rho_j g[z - z_0(r)] - \epsilon \rho_j \left\{ \frac{\partial \phi_j}{\partial t} + \frac{1}{4\Omega^2} \frac{\partial^3 \phi_j}{\partial t^3} \right\} \tag{6}$$

for $j = 1,2$.

Substitution of (5) and (6) into (1) shows that the rotating Euler equation is satisfied at leading order by the order 1 hydrostatic pressure terms and at order ϵ by the generalized potential ϕ. (We note that both the present formulation and that of Miles [13,14] necessarily imply a swirl component to the flow as soon as the radial velocity is nonzero.) By further assuming that the fluid in each layer is incompressible, i.e., $\nabla \cdot \boldsymbol{u}_j = 0$, we obtain the governing wave equation for each fluid layer

$$\left\{ \partial_t^2 \nabla^2 + 4\Omega^2 \partial_z^2 \right\} \phi_j = 0, \quad j = 1,2. \tag{7}$$

Solutions to this type of wave equation in the context of inertial waves and internal gravity waves are well known (see, e.g., [19] and references therein).

We seek to solve the governing equation (7) together with the following boundary conditions: that there is no flow through the tank walls, an impermeability condition given by

$$\boldsymbol{u} \cdot \boldsymbol{e}_r = 0 \quad \text{on } r = a,$$
$$\boldsymbol{u} \cdot \boldsymbol{e}_z = 0 \quad \text{on } z = \pm d; \tag{8}$$

we also require that the velocity on the axis of rotation $r = 0$ is sufficiently regular, specifically that

$$r \partial \phi_j^2 / \partial r \to 0 \quad \text{as } r \to 0 \tag{9}$$

(this condition allows for finite fluid velocities across the axis of rotation); and finally, we require continuity of stress across the interface. In the absence of viscosity we therefore require

$$p|_-^+ = 0 \quad \text{across } z = z_0(r) + \epsilon \zeta(r,\theta,t). \tag{10}$$

Since ζ is unknown we require the kinematic condition that the interface moves with the local fluid velocity to close the system:

$$\frac{D}{Dt}(z_0 + \epsilon \zeta) = \boldsymbol{u} \cdot \boldsymbol{e}_z \quad \text{on } z = z_0(r) + \epsilon \zeta(r,\theta,t). \tag{11}$$

Following Taylor [2] and Miles [14] we adopt a variational formulation and seek normal mode solutions of the form

$$\phi = \hat{\phi}(r,z) \exp\{i(\omega t + m\theta)\}, \quad \zeta = \hat{\zeta}(r) \exp\{i(\omega t + m\theta)\}, \tag{12}$$

where $m \in \mathbb{N}_0$ is an azimuthal wave number. Substitution into (7) yields the governing equation

$$\frac{1}{r} \frac{\partial}{\partial r} \left(r \frac{\partial \hat{\phi}_j}{\partial r} \right) - \frac{m^2}{r^2} \hat{\phi}_j + (1 - \mu^2) \frac{\partial^2 \hat{\phi}_j}{\partial z^2} = 0, \quad j = 1,2, \tag{13}$$

where we adopt Miles' [14] notation by defining $\mu = 2\Omega/\omega$. The boundary conditions (8) and (9) become

$$r \partial \hat{\phi}_j^2 / \partial r \to 0 \quad \text{as } r \to 0,$$
$$r \partial \hat{\phi}_j / \partial r + \mu m \hat{\phi}_j = 0 \quad \text{on } r = a, \tag{14}$$
$$\partial \hat{\phi}_j / \partial z = 0 \quad \text{on } z = \pm d,$$

where the plus or minus is taken according to whether $j = 1$ or 2, respectively. The condition of pressure continuity across the interface (10) yields, at order ϵ,

$$i\omega \mu^2 \hat{\zeta} = \frac{2\Omega^2}{g} \left(1 - \frac{1}{\mu^2} \right) \left(\frac{1 + \mathscr{A}}{\mathscr{A}} \hat{\phi}_2 - \frac{1 - \mathscr{A}}{\mathscr{A}} \hat{\phi}_1 \right) \tag{15}$$

on $z = z_0(r)$. The kinematic condition (11) at order ϵ can be written as

$$i\omega\mu^2\hat{\zeta} = z_0'\left(\frac{\partial\hat{\phi}_j}{\partial r} + \frac{\mu m}{r}\hat{\phi}_j\right) - (1-\mu^2)\frac{\partial\hat{\phi}_j}{\partial z}, \quad j = 1,2 \tag{16}$$

on $z = z_0(r)$ for each layer, where $z_0' \equiv dz_0/dr$.

The variational functional $\Phi[\hat{\phi}_1, \hat{\phi}_2]$ is defined by multiplying the governing equation (13) by $\rho_j\hat{\phi}_j$ and integrating over the domain $\mathscr{D} = \mathscr{D}_1 \cup \mathscr{D}_2 = [0,a] \times [-d,d]$ (see Fig. 2) so that

$$\Phi = \int_{\mathscr{D}} \rho\hat{\phi}\left\{\frac{1}{r}\frac{\partial}{\partial r}\left(r\frac{\partial\hat{\phi}}{\partial r}\right) - \frac{m^2}{r^2}\hat{\phi} + (1-\mu^2)\frac{\partial^2\hat{\phi}}{\partial z^2}\right\}dA. \tag{17}$$

Following the method outlined by Miles [14], we write the integral (17) in conservative form, giving

$$\Phi = \int_{\mathscr{D}} \rho\left[\frac{1}{r}\frac{\partial}{\partial r}\left(r\hat{\phi}\frac{\partial\hat{\phi}}{\partial r}\right) + (1-\mu^2)\frac{\partial}{\partial z}\left(\hat{\phi}\frac{\partial\hat{\phi}}{\partial z}\right)\right]dA$$
$$- \int_{\mathscr{D}} \rho\left[\left(\frac{\partial\hat{\phi}}{\partial r}\right)^2 + \frac{m^2}{r^2}\hat{\phi}^2 + (1-\mu^2)\left(\frac{\partial\hat{\phi}}{\partial z}\right)^2\right]dA. \tag{18}$$

We consider the first integral in Eq. (18) and integrate over $\mathscr{D}_1$ and $\mathscr{D}_2$ separately. Defining I_1 to be the integral over $\mathscr{D}_1$ and I_2 to be the integral over $\mathscr{D}_2$, we have

$$I_1 = \int_{z_0(0)}^{z_0(a)} \int_0^{r_0(z)} \frac{\rho_1}{r}\frac{\partial}{\partial r}\left(r\hat{\phi}_1\frac{\partial\hat{\phi}_1}{\partial r}\right)r\,dr\,dz + \int_{z_0(a)}^d \int_0^a \frac{\rho_1}{r}\frac{\partial}{\partial r}\left(r\hat{\phi}_1\frac{\partial\hat{\phi}_1}{\partial r}\right)r\,dr\,dz$$
$$+ \int_0^a \int_{z_0(r)}^d \rho_1(1-\mu^2)\frac{\partial}{\partial z}\left(\hat{\phi}_1\frac{\partial\hat{\phi}_1}{\partial z}\right)r\,dz\,dr, \tag{19}$$

where $r_0(z)$ is the well-defined inverse of $z_0(r)$. Integrating and enforcing the boundary conditions $\partial\hat{\phi}_1/\partial z|_{z=d} = 0$, $(r\partial\hat{\phi}_1/\partial r + \mu m\hat{\phi}_1)|_{r=a} = 0$, and $r\partial\hat{\phi}_1^2/\partial r \to 0$ as $r \to 0$ implies

$$I_1 = \rho_1 \int_{z_0(0)}^{z_0(a)} r\hat{\phi}_1\frac{\partial\hat{\phi}_1}{\partial r}\bigg|_{r=r_0(z)} dz - \rho_1\mu m \int_{z_0(a)}^d \hat{\phi}_1^2|_{r=a}dz - \rho_1(1-\mu^2)\int_0^a \hat{\phi}_1\frac{\partial\hat{\phi}_1}{\partial z}\bigg|_{z=z_0(r)} r\,dr. \tag{20}$$

Transforming the first term in Eq. (20) by making the substitution $z = z_0(r)$ gives the result

$$I_1 = -\rho_1\mu m \int_{z_0(a)}^d \hat{\phi}_1^2\bigg|_{r=a} dz + \rho_1 \int_0^a \hat{\phi}_1\left\{z_0'\frac{\partial\hat{\phi}_1}{\partial r} - (1-\mu^2)\frac{\partial\hat{\phi}_1}{\partial z}\right\}\bigg|_{z=z_0(r)} r\,dr. \tag{21a}$$

Following a similar procedure, we may also show

$$I_2 = -\rho_2\mu m \int_{-d}^{z_0(a)} \hat{\phi}_2^2\bigg|_{r=a} dz - \rho_2 \int_0^a \hat{\phi}_2\left\{z_0'\frac{\partial\hat{\phi}_2}{\partial r} - (1-\mu^2)\frac{\partial\hat{\phi}_2}{\partial z}\right\}\bigg|_{z=z_0(r)} r\,dr. \tag{21b}$$

Eliminating the interface perturbation ζ from the pressure continuity condition (15) and the kinematic condition (16), we see that

$$z_0'\frac{\partial\hat{\phi}_j}{\partial r} - (1-\mu^2)\frac{\partial\hat{\phi}_j}{\partial z} = -z_0'\frac{\mu m}{r}\hat{\phi}_j + \frac{2\Omega^2}{g}\left(1 - \frac{1}{\mu^2}\right)\left(\frac{1+\mathscr{A}}{\mathscr{A}}\hat{\phi}_2 - \frac{1-\mathscr{A}}{\mathscr{A}}\hat{\phi}_1\right) \tag{22}$$

for $j = 1,2$ on $z = z_0(r)$. Thus, we may rewrite (21a) and (21b) as

$$
I_1 = -\rho_1 \mu m \int_{z_0(a)}^{d} \hat{\phi}_1^2 \Big|_{r=a} dz
$$

$$
+ \int_0^a \rho_1 \hat{\phi}_1 \left\{ \frac{2\Omega^2}{g} \left(1 - \frac{1}{\mu^2}\right) \left(\frac{1+\mathscr{A}}{\mathscr{A}}\hat{\phi}_2 - \frac{1-\mathscr{A}}{\mathscr{A}}\hat{\phi}_1\right) - z_0' \frac{\mu m}{r}\hat{\phi}_1 \right\} \Big|_{z=z_0(r)} r\, dr, \quad (23a)
$$

$$
I_2 = -\rho_2 \mu m \int_{-d}^{z_0(a)} \hat{\phi}_2^2 \Big|_{r=a} dz
$$

$$
- \int_0^a \rho_2 \hat{\phi}_2 \left\{ \frac{2\Omega^2}{g} \left(1 - \frac{1}{\mu^2}\right) \left(\frac{1+\mathscr{A}}{\mathscr{A}}\hat{\phi}_2 - \frac{1-\mathscr{A}}{\mathscr{A}}\hat{\phi}_1\right) - z_0' \frac{\mu m}{r}\hat{\phi}_2 \right\} \Big|_{z=z_0(r)} r\, dr. \quad (23b)
$$

Substituting (23) into (18), we have that

$$
\Phi[\phi_1, \phi_2] = -\rho_1 \mu m \int_{z_0(a)}^{d} \hat{\phi}_1^2\big|_{r=a} dz - \rho_2 \mu m \int_{-d}^{z_0(a)} \hat{\phi}_2^2\big|_{r=a} dz
$$

$$
+ \int_0^a \rho_1 \hat{\phi}_1 \left\{ \frac{2\Omega^2}{g} \left(1 - \frac{1}{\mu^2}\right) \left(\frac{1+\mathscr{A}}{\mathscr{A}}\hat{\phi}_2 - \frac{1-\mathscr{A}}{\mathscr{A}}\hat{\phi}_1\right) - z_0' \frac{\mu m}{r}\hat{\phi}_1 \right\} \Big|_{z=z_0(r)} r\, dr
$$

$$
- \int_0^a \rho_2 \hat{\phi}_2 \left\{ \frac{2\Omega^2}{g} \left(1 - \frac{1}{\mu^2}\right) \left(\frac{1+\mathscr{A}}{\mathscr{A}}\hat{\phi}_2 - \frac{1-\mathscr{A}}{\mathscr{A}}\hat{\phi}_1\right) - z_0' \frac{\mu m}{r}\hat{\phi}_2 \right\} \Big|_{z=z_0(r)} r\, dr
$$

$$
- \int_{\mathscr{D}_1} \rho_1 \left[\left(\frac{\partial \hat{\phi}_1}{\partial r}\right)^2 + \frac{m^2}{r^2}\hat{\phi}_1^2 + (1-\mu^2)\left(\frac{\partial \hat{\phi}_1}{\partial z}\right)^2 \right] dA
$$

$$
- \int_{\mathscr{D}_2} \rho_2 \left[\left(\frac{\partial \hat{\phi}_2}{\partial r}\right)^2 + \frac{m^2}{r^2}\hat{\phi}_2^2 + (1-\mu^2)\left(\frac{\partial \hat{\phi}_2}{\partial z}\right)^2 \right] dA. \quad (24)
$$

Taking the functional derivative of Φ with respect to, for example, $\hat{\phi}_1$, where $\delta_1 \Phi \equiv \Phi[\hat{\phi}_1 + \delta\hat{\phi}_1, \hat{\phi}_2] - \Phi[\hat{\phi}_1, \hat{\phi}_2]$, yields, after some manipulation,

$$
\delta_1 \Phi = 2\rho_1 \int_{\mathscr{D}_1} \left\{ \frac{1}{r}\frac{\partial}{\partial r}\left(r\frac{\partial \hat{\phi}_1}{\partial r}\right) - \frac{m^2}{r^2}\hat{\phi}_1 + (1-\mu^2)\frac{\partial^2 \hat{\phi}_1}{\partial z^2} \right\} \delta\hat{\phi}_1 dA
$$

$$
- 2\rho_1 \int_{z_0(a)}^{d} \left\{ \mu m \hat{\phi}_1 + r\frac{\partial \hat{\phi}_1}{\partial r} \right\} \delta\hat{\phi}_1 \Big|_{r=a} dz
$$

$$
+ 2\rho_1 \int_0^a \left\{ \frac{2\Omega^2}{g}\left(1 - \frac{1}{\mu^2}\right)\left(\frac{1+\mathscr{A}}{\mathscr{A}}\hat{\phi}_2 - \frac{1-\mathscr{A}}{\mathscr{A}}\hat{\phi}_1\right) \right.
$$

$$
\left. - z_0'\frac{\mu m}{r}\hat{\phi}_1 - \left[z_0'\frac{\partial \hat{\phi}_1}{\partial r} - (1-\mu^2)\frac{\partial \hat{\phi}_1}{\partial z} \right] \right\} \delta\hat{\phi}_1 \Big|_{z=z_0(r)} r\, dr. \quad (25)
$$

So we see that the functional Φ is stationary with respect to first-order variations of $\hat{\phi}_1$ about the solution of the governing equation (13) in $\mathscr{D}_1$, the boundary condition (22) for $j = 1$ at the interface $z = z_0(r)$ and at the no-radial flow condition at $r = a$ on the boundary of $\mathscr{D}_1$. Similarly, Φ is stationary

with respect to first-order variations of $\hat{\phi}_2$ about the solution of the governing equation (13) in $\mathscr{D}_2$, the boundary condition (22) for $j = 2$ at the interface $z = z_0(r)$ and the no-radial flow condition at $r = a$ on the boundary of $\mathscr{D}_2$. [The Euler-Lagrange equation for Φ as expressed in Eq. (17) is the governing equation (13) multiplied by $2\rho_j$.] Following Miles [14], we pose trial solutions that satisfy the governing equation (13), the regularity condition at $r = 0$, and the boundary conditions on $r = a$ and $z = \pm d$ exactly and invoke the variational principle only with respect to the final boundary condition on $z = z_0(r)$.

If $\hat{\phi}$ is an exact solution of the governing equation (13), it follows from the definition of Φ that $\Phi(\hat{\phi}) = 0$. Therefore, if $\hat{\phi}$ is a solution of (13), it follows from (18) and (21) that

$$\int_{\mathscr{D}} \rho \left[\left(\frac{\partial \hat{\phi}}{\partial r} \right)^2 + \frac{m^2}{r^2} \hat{\phi}^2 + (1 - \mu^2) \left(\frac{\partial \hat{\phi}}{\partial z} \right)^2 \right] dA$$

$$= -\rho_1 \mu m \int_{z_0(a)}^{d} \hat{\phi}_1^2 \bigg|_{r=a} dz - \rho_2 \mu m \int_{-d}^{z_0(a)} \hat{\phi}_2^2 \bigg|_{r=a} dz$$

$$+ \int_0^a \rho_1 \hat{\phi}_1 \left\{ z_0' \frac{\partial \hat{\phi}_1}{\partial r} - (1 - \mu^2) \frac{\partial \hat{\phi}_1}{\partial z} \right\} \bigg|_{z=z_0(r)} r \, dr$$

$$- \int_0^a \rho_2 \hat{\phi}_2 \left\{ z_0' \frac{\partial \hat{\phi}_2}{\partial r} - (1 - \mu^2) \frac{\partial \hat{\phi}_2}{\partial z} \right\} \bigg|_{z=z_0(r)} r \, dr. \tag{26}$$

Substituting (26) into (24), we therefore have, after simplification,

$$\Phi \propto \int_0^a \left\{ \omega^2 \left[\frac{1 + \mathscr{A}}{\mathscr{A}} \hat{\phi}_2 - \frac{1 - \mathscr{A}}{\mathscr{A}} \hat{\phi}_1 \right]^2 + \left[\frac{\Omega^2}{1 - \mu^2} \left(r \frac{\partial}{\partial r} + 2\mu m \right) - g \frac{\partial}{\partial z} \right] \right.$$

$$\left. \times \left[\frac{1 + \mathscr{A}}{\mathscr{A}} \hat{\phi}_2^2 - \frac{1 - \mathscr{A}}{\mathscr{A}} \hat{\phi}_1^2 \right] \right\} \bigg|_{z=z_0(r)} r \, dr. \tag{27}$$

The constant of proportionality is $(\rho_2 - \rho_1)(1 - \mu^2)/4g$, but as interest is focused upon stationary values of Φ, it will be disregarded. The expression in Eq. (27) is the two-layer equivalent of the functional given in (3.2) of Ref. [14] and it can be seen that Miles' expression is recovered in the limit $\mathscr{A} = 1$ (the stable single layer limit). The cross term in the first term of the integrand is crucial in coupling the behavior of the two fluid layers.

Again, following Miles [14], we seek to construct a series solution based on trial solutions of the form

$$\hat{\phi}_{jn}(r,z) = \mathscr{J}_m \left(\frac{k_n r}{a} \right) \cosh \left(\frac{k_n}{a} \frac{[z \mp d]}{\sqrt{1 - \mu^2}} \right) \tag{28}$$

for $n = 1, 2, \ldots$, where $\mathscr{J}_m$ is a Bessel function of the first kind and we take the minus or plus sign in Eq. (28) according to whether $j = 1$ or 2, respectively. The trial solutions (28) satisfy both the governing equation (13) and the vertical impermeability boundary conditions at $z = \pm d$. The radial impermeability boundary condition at $r = a$ sets the possible modes of solution and so in general we sum over the countable number of solutions k_n of

$$k \mathscr{J}_{m+1}(k) = m(1 + \mu) \mathscr{J}_m(k), \tag{29}$$

which follows from substituting (28) into (14) and setting $r = a$. (The ratio k_n/a may be regarded as the radial wave number associated with the nth mode.) The trial solutions (28) form a complete set over $\mathscr{D}$ (and are orthogonal in each layer when $\mu = 0$) and so as the number of terms in the series increases we approach a full solution [14]. (See Ref. [20] for a description of this classical approach

and its relation to the method of weighted residuals.) Thus, we approximate $\hat{\phi}_1$ and $\hat{\phi}_2$ by

$$\hat{\phi}_j \approx \hat{\phi}_j^{(N)} = \sum_{n=1}^{N} c_{jn} \hat{\phi}_{jn}, \quad j = 1,2 \text{ for some } N \geqslant 1. \tag{30}$$

We adopt a variational approach applied to (27) in order to find the coefficients c_{jn} such that our solution satisfies (22) on $z = z_0(r)$, the remaining unsatisfied condition. Specifically, by seeking stationary values of the functional Φ, by taking the partial derivatives $\partial\Phi/\partial c_{jn}$, $j = 1,2$, $n = 1,\dots,N$, we may construct $2N$ linear equations in the $2N$ coefficients. The eigenvalue equation for ω is found by setting the determinant of this linear system to be zero. If ω has a negative imaginary part, then (12) implies growth and the onset of the Rayleigh-Taylor instability.

In the remainder of this section we initially consider purely axisymmetric instabilities, first asymptotically for low rotation rates in Secs. II B 1–II B 3 and then numerically for arbitrary rotation rates in Sec. II B 4. We then consider asymmetric instabilities, first asymptotically for low rotation rates in Secs. II C 1–II C 3 and then numerically for arbitrary rotation rates in Secs. II C 4 and II C 5.

B. Axisymmetric instability $m = 0$

In the first instance we consider purely axisymmetric motion: the special case $m = 0$. Setting $m = 0$ in Eq. (29) shows that we sum over the zeros of $\mathcal{J}_1(k)$, which implies $k \in \mathbb{R}$.

1. Single-mode, low-rotation-rate, gravity wave solutions: Asymptotics

Following Miles [14], we initially consider a solution containing a single trial solution, each in the upper and lower layers. We further assume a low rotation rate such that $\alpha = \Omega^2 a/g \ll 1$. Using such an approximation, Miles was able to explain the discrepancies between the theory of Lamb [15] and the experimental observations of Fultz (see [6], Fig. 12) and so we adopt this level of approximation for initial investigation. Seeking an asymptotic expression for the eigenvalue equation for ω, we take (28) for some single $n \in \mathbb{N}$. By considering $\partial\Phi/\partial c_{1n} = 0$ and $\partial\Phi/\partial c_{2n} = 0$ and expanding in powers of α we find, after some significant manipulation, that an eigenvector of the solution is

$$\boldsymbol{c} \propto \left[1, -1 - \tfrac{1}{6}\coth(k_n\delta)\alpha + O(\alpha^2) \right], \tag{31}$$

where $\delta = d/a$, and the eigenvalue equation for ω is

$$\omega^2 \sim g\mathscr{A}\frac{k_n}{a}\tanh(k_n\delta) + 2\Omega^2 \left[1 + 2k_n\delta\,\mathrm{csch}(2k_n\delta) - \frac{1}{24}k_n^2\mathscr{A}^2\mathrm{sech}^2(k_n\delta) \right] + \frac{g}{a}O(\alpha^2). \tag{32}$$

We observe therefore that if $g\mathscr{A} < 0$, then $\omega^2 < 0$ and interfacial perturbations will grow rather than oscillate: the Rayleigh-Taylor instability. The form of (32) suggests that we may be able to suppress this growth to some extent by rotating the system, i.e., the second term in Eq. (32) may be used to compete with the first if it has the opposing sign. However, it would be mistaken to suggest that (32) implies that, given a sufficient rotation rate, an unstable mode could be fully stabilized ($\omega^2 > 0$), as is concluded erroneously by Sharma *et al.* [21] in the context of particle laden Rayleigh-Taylor instability. The expansion (32) is asymptotic and its validity breaks down when the second term is comparable to the first. The correct approach is to consider an expansion when ω, not Ω, is small compared to $(a/g)^{1/2}$ (see Sec. II B 3). The expression in Eq. (32) is the first of two key results we present. It is the dispersion relation for a slowly rotating two-layer fluid system that may be either stably stratified or Rayleigh-Taylor unstable.

Whether the growth rate of a given wave mode is reduced or increased by rotation depends on the sign of the second term in Eq. (32). Provided $|\mathscr{A}|/\delta \lesssim 8.72$, then there are no solutions for which the second term in Eq. (32) can be made negative and so the effect of rotation is always to initially suppress a given wave mode. (The threshold coefficient $c \approx 8.72$ is given by

$$c^2 = \frac{24}{\xi_0^2}[\xi_0\coth\xi_0 + \cosh^2\xi_0],$$

where

$$\xi_0[\sinh(4\xi_0) - 2\xi_0] = 2[\sinh(2\xi_0) + \xi_0]^2,$$

giving $\xi_0 \approx 1.39$) However, if $|\mathscr{A}|/\delta \gtrsim 8.72$, indicating a sufficiently strong stratification or sufficiently shallow aspect ratio, then there may exist wave modes that are excited by rotating the system. For example, $\mathscr{A} = -\frac{1}{2}$, $\delta = \frac{1}{18}$, and $n = 7$ gives $|\mathscr{A}|/\delta = 9 > c$, $k_7 \approx 22.76$, and the second term of (32) is approximately -0.14, i.e., the seventh mode is excited rather than suppressed as the first six modes are.

Rather than considering the limit of low rotation rate $\alpha \ll 1$, we may substitute (28) into (27) with $m = 0$ and take $\delta \to \infty$, which may be thought of as forcing a horizontal initial interface, rather than parabolic, to find

$$\omega^4 - 4\Omega^2\omega^2 - \omega_0^4 = 0 \quad \text{where} \quad \omega_0^2 = g\mathscr{A}\frac{k_n}{a}, \tag{33}$$

the solution of which, selecting the physically appropriate branch by introducing the factor $\mathscr{A}/|\mathscr{A}|$, is Chandrasekhar's solution [see Eqs. (162) and (163) in Ref. [16]], given by

$$\omega^2 = 2\Omega^2 + \frac{\mathscr{A}}{|\mathscr{A}|}\sqrt{4\Omega^4 + \omega_0^4} \tag{34}$$

in the present notation.

If the vertical coordinate z is scaled by the layer depth d and the radial coordinate r is scaled by the domain radius a, then the nondimensional form of (3) is

$$z_0^\star(r^\star) = \frac{\alpha}{2\delta}\left(r^{\star 2} - \frac{1}{2}\right), \tag{35}$$

where superscript stars denote nondimensional quantities. It follows from (35) that for the interface between the two fluid layers to be horizontal, i.e., $z_0^\star(r^\star) = $ const, then either $\alpha = 0$ and the system is not rotating or we are considering the limit $\delta \to \infty$. Hence we may interpret the approximation of Chandrasekhar [16], that the system is rotating, but has a horizontal initial interface, as considering the special case of $d \to \infty$ and $a \to \infty$, with infinite aspect ratio $\delta \to \infty$. We can expect therefore that when we have large aspect ratio δ and moderate values of α, (34) will be a better approximation to ω than the asymptotic expansion (32) since no small rotation rate approximation has been made in the case of (34). [We note that the two solutions (32) and (34) coincide, as they must, if $\delta \gg 1$ and $\alpha \ll 1$.]

2. Single-mode, low-rotation-rate, inertial wave solutions: Asymptotics

We show the presence of inertial waves when $\omega^2 \sim O(\alpha)$. We consider $\partial\Phi/\partial c_{1,n} = 0$ and $\partial\Phi/\partial c_{2,n} = 0$ for a single $n \in \mathbb{N}$, but specifically seek solutions for which ω^2 does not have an order 1 contribution, but has a leading-order contribution at $O(\alpha)$.

In order to ensure that ω^2 has no leading-order contribution we find that we must satisfy

$$\sinh\left(\frac{2k_n\delta}{\sqrt{1-\mu^2}}\right) \sim O(\alpha), \tag{36}$$

which requires

$$\frac{\omega^2 a}{g} \sim \frac{4\alpha}{1 + [2k_n\delta_q]^2} + O(\alpha^2), \tag{37}$$

where $\delta_q = \delta/q\pi$ for $\pm q = 1, 2, \ldots$. The frequencies associated with these wave modes depend upon whether q is even or odd. For q odd

$$\frac{\omega^2 a}{g} \sim \frac{4\alpha}{1 + [2k_n\delta_q]^2}\left\{1 \mp \frac{[2k_n\delta_q]^2}{1 + [2k_n\delta_q]^2}\frac{\alpha}{6\delta} + O(\alpha^2)\right\}, \tag{38}$$

where the minus or plus sign is taken according to whether the wave occurs mainly in the upper or lower fluid, respectively. The eigenvectors correspond to waves occurring in either predominantly the upper fluid $\boldsymbol{c} = (1, O(\alpha^2))$ or predominantly the lower fluid $\boldsymbol{c} = (O(\alpha^2), 1)$.

For q even,

$$\frac{\omega^2 a}{g} \sim \frac{4\alpha}{1 + [2k_n\delta_q]^2}\Bigg[1 - \frac{[2k_n\delta_q]^2}{(1 + [2k_n\delta_q]^2)^2}\frac{1}{\mathscr{A}}\bigg((4\delta_q)^2$$

$$\pm \frac{1}{6}((1 + [2k_n\delta_q]^2)\{1 + [2k_n\delta_q]^2 - 12(4\delta_q)^2\}\mathscr{A}^2 + 36(4\delta_q)^4)^{1/2}\bigg)\frac{\alpha}{\delta} + O(\alpha^2)\Bigg]. \tag{39}$$

It is straightforward to show that when $\mathscr{A} = 1$, δ_q is replaced by $\delta_q/2$, and the minus sign is chosen in Eq. (39) (corresponding to the flow taking place in the lower fluid), the solution in (4.13) in Ref. [14] is recovered. The solutions Miles found correspond to the even q solutions; hence δ_q must be replaced by $\delta_q/2$ above for comparison. For even q the associated eigenvector is

$$\boldsymbol{c} = \Bigg(1, \frac{1}{6(1 + \mathscr{A})(4\delta_q)^2}[\mathscr{A}\{1 + [2k_n\delta_q]^2 - 6(4\delta_q)^2\}$$

$$\mp (\mathscr{A}^2(1 + [2k_n\delta_q]^2)\{1 + [2k_n\delta_q]^2 - 12(4\delta_q)^2\} + 36(4\delta_q)^4)^{1/2}] + O(\alpha)\Bigg). \tag{40}$$

The odd q solutions are present for all values of $\mathscr{A}$ including the special case $\mathscr{A} = 1$.

3. Single-mode critical rotation rate for stabilization

A critical rotation rate Ω_c for which a single gravity wave mode is stable for $\Omega > \Omega_c$ and unstable for $\Omega < \Omega_c$ can be found by considering an asymptotic expansion of Φ as a series in $\omega^2 a/g$. Near the stability threshold we are in a regime $\omega^2 a/g \ll 1$ and thus an expansion to the first two terms of the series can be used to find the critical rotation rate.

We have that for $m = 0$, k_n is such that $\mathcal{J}_1(k_n) = 0$ and so using the results

$$\int_0^1 \frac{\mathcal{J}_0^2(k_n x)}{\mathcal{J}_0^2(k_n)} x\, dx = \frac{1}{2}, \tag{41a}$$

$$\int_0^1 \frac{\mathcal{J}_0^2(k_n x)}{\mathcal{J}_0^2(k_n)} x^3 dx = \frac{1}{6}, \tag{41b}$$

$$\int_0^1 \mathcal{J}_0(k_n x)\mathcal{J}_1(k_n x) x^2 dx = 0, \tag{41c}$$

we may show that if $\alpha = \alpha_0 + a\omega^2\alpha_1/g + \cdots$, to leading order the variational function Φ is proportional to

$$\frac{\omega^2 a}{g}\left\{\left[\frac{1 - \mathscr{A}}{\mathscr{A}}c_{1n} - \frac{1 + \mathscr{A}}{\mathscr{A}}c_{2n}\right]^2 + \frac{1 - \mathscr{A}}{2\mathscr{A}}\left[\frac{k_n^2}{12} + \frac{\delta k_n^2}{\alpha_0}\right]c_{1n}^2 - \frac{1 + \mathscr{A}}{2\mathscr{A}}\left[\frac{k_n^2}{12} - \frac{\delta k_n^2}{\alpha_0}\right]c_{2n}^2\right\}. \tag{42}$$

It follows that for nontrivial solutions of $\partial\Phi/\partial c_{1n} = 0$ and $\partial\Phi/\partial c_{2n} = 0$ we require to leading order

$$\left\{\frac{1 - \mathscr{A}}{\mathscr{A}} + \frac{1}{2}\left[\frac{k_n^2}{12} + \frac{\delta k_n^2}{\alpha_0}\right]\right\}\left\{\frac{1 + \mathscr{A}}{\mathscr{A}} - \frac{1}{2}\left[\frac{k_n^2}{12} - \frac{\delta k_n^2}{\alpha_0}\right]\right\} - \frac{1 - \mathscr{A}^2}{\mathscr{A}^2} = 0, \tag{43}$$

at the instability threshold $\omega = 0$ and hence $\alpha = \alpha_0$. Thus, we may solve (43) for $\alpha_0 = \alpha_c$, the critical value of α that yields $\omega = 0$. Hence, we find the critical rotation rate Ω_c to be given exactly by

$$\frac{\Omega_c^2 a}{g} = \frac{6\delta}{\mathscr{A}}\left(1 - \frac{k_n^2}{48}\right)^{-1}\left[\left\{1 - \frac{k_n^2 \mathscr{A}^2}{12}\left(1 - \frac{k_n^2}{48}\right)\right\}^{1/2} - 1\right]. \tag{44}$$

This result does not depend on exploiting a small rotation rate or other small external parameter and so is not asymptotic and is therefore true in general. Since $\Omega_c \in \mathbb{R}$, (44) only applies for $-1 \leqslant \mathscr{A} < 0$, i.e., a critical rotation rate only exists if the fluid layers would be Rayleigh-Taylor unstable in a nonrotating regime, as might be anticipated on physical grounds. Under this condition on $\mathscr{A}$, (44) can be shown to be a strictly monotonically increasing function in k_n, bounded such that $\alpha_c \in [0, 12\delta)$.

A key observation from (44) is that the monotonic dependence of α_c on k_n means that for a given rotation rate all structures larger than the critical wavelength associated with k_n are stabilized, whereas all structures smaller than the critical wavelength remain unstable. This is in keeping with the physical arguments presented earlier in the Introduction.

There exists a threshold rotation rate $\alpha = 4\delta$, where the hydrostatic interface intersects the lid and the base of the domain and, as a result, the assumed form of ϕ no longer satisfies the boundary conditions at $z = \pm d$. So, although it follows from (44) that for a given radial wave number k_n there exists a critical rotation rate for stabilization, it is not guaranteed that this critical rotation rate is less than the threshold rotation rate 4δ. That is to say, although (44) implies that since there are no growing axisymmetric modes for $-1 \leqslant \mathscr{A} < 0$ when $\Omega_c^2 a/g > 12\delta$, suggesting all axisymmetric modes may therefore be made indefinitely stable, this absolute critical rotation rate cannot be attained before the model breaks down. In summary, (44) shows that for a given rotation rate there exists a critical wavelength, above which all axisymmetric modes are stable, but below which all short wavelength modes remain unstable.

Chandrasekhar (see Chap. X, Sec. 95 in Ref. [16]) considers the special case of a two-layer stratification of semi-infinite fluids with a horizontal interface and states that "... it follows that in the present case rotation does not affect the instability or stability, as such, of a stratification ..." The critical rotation rate given in Eq. (44) shows that Chandrasekhar's result is a special case and not true in general for purely axisymmetric flows, supporting Carnevale *et al.* [22]. The case of two semi-infinite fluids superposed is given by taking the limits $a \to \infty$ and $d \to \infty$. The assumption of a horizontal interface implies that these limits should be taken such that $\delta = d/a \to \infty$. Taking the limit $\delta \to \infty$ in Eq. (44) shows that there is indeed no finite critical rotation rate to stabilize a given unstable mode as $\delta \to \infty$ since $\Omega_c \to \infty$. The result (44) is the second key result presented here and shows that, for finite-aspect-ratio flows, it is possible to completely suppress some Rayleigh-Taylor unstable modes by rotating the system.

4. Single-mode, arbitrary-rotation-rate solutions: Numerics

In order to obtain results at arbitrary rotation rate we proceed using a hybrid of analytical and numerical methods, whereby evaluation of integrals is carried out using Simpson's rule. For $N = 1$ and $n = 1$ we construct the matrix of coefficients of c_{jn} from the linear equations $\partial \Phi / \partial c_{jn} = 0$ for $j = 1, 2$. This yields a 2×2 matrix M and the zeros of its determinant, corresponding to possible solutions, are calculated numerically and plotted in Fig. 3 for $\mathscr{A} = \pm\frac{1}{2}$ and $\delta = \frac{1}{4}, 4$. The zero-rotation-rate solutions, as found by Taylor [2], are indicated by white circles on the vertical axes. Selecting $n = 1$ gives $k = k_1$, the first zero of $\mathcal{J}_1$, and so we have $k \approx 3.83$.

Inertial waves are present as a result of the rotation and it can be seen that these solutions all converge at the origin, indicating that as the rotation rate tends to zero these waves are not supported, consistent with their definition. The first pair of inertial wave solutions, corresponding to (38) with $q = 1$, are indicated by dot-dashed lines extending away from the origin. The grayed-out regions
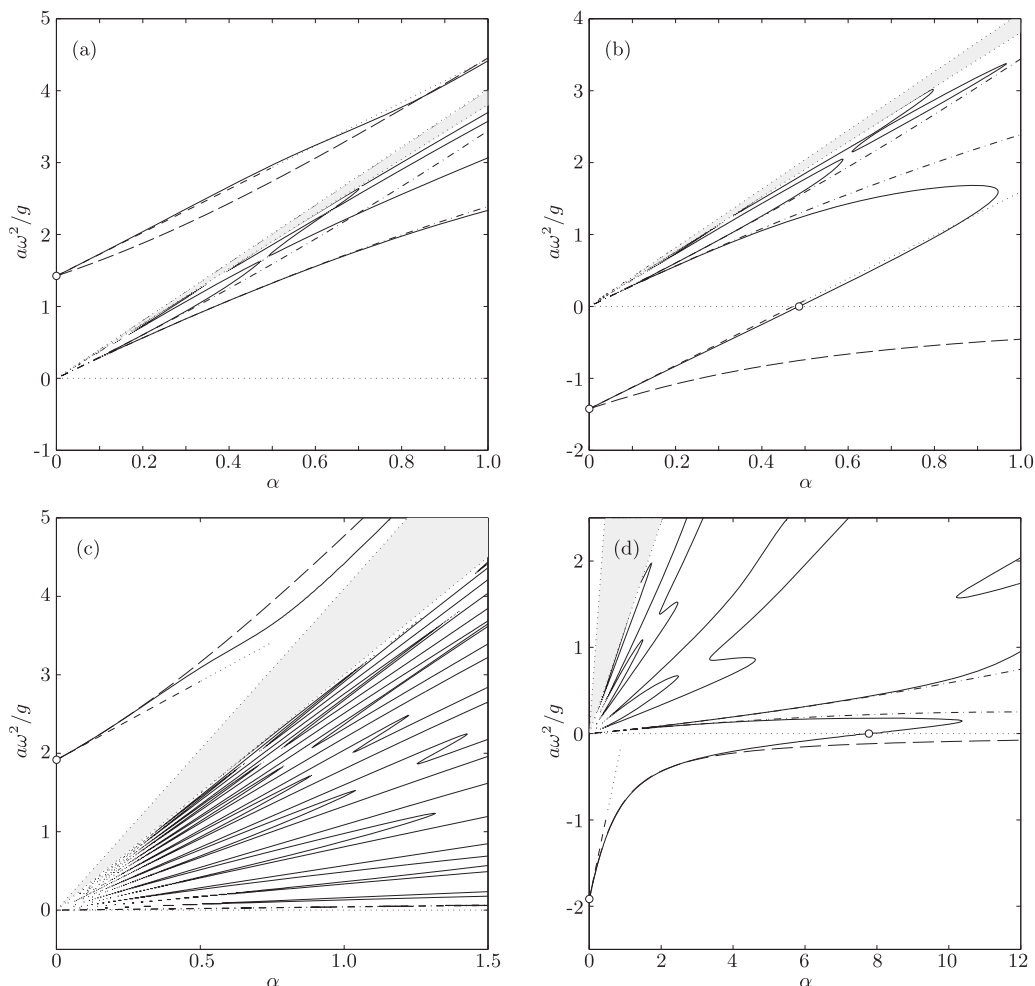
FIG. 3. Solutions of the eigenvalue problem, consistent with the assumptions of Sec. II A, describing the dispersion relation for Atwood numbers $\mathscr{A} = \pm\frac{1}{2}$ (stable and unstable, respectively), $\delta = \frac{1}{4}, 4$, $N = 1$, and $k = k_1 \approx 3.83$. Solid lines are the exact solution calculated numerically. The long-dashed lines correspond to Chandrasekhar's solution (34). (a) Stable: $\mathscr{A} = \frac{1}{2}$ and $\delta = \frac{1}{4}$. The gravity wave solution coincides with the $\alpha = 0$ axis at the value given by Taylor, indicated by a circle. The asymptotic solution is shown as a dashed line for $\alpha < 0.5$ and continues as dotted for larger values. The first pair of inertial wave solutions (38) corresponding to $q = 1$ are shown (dot-dashed lines). The grayed region contains an infinite number of possible inertial wave solutions corresponding to higher values of q. (b) Unstable: $\mathscr{A} = -\frac{1}{2}$ and $\delta = \frac{1}{4}$. On $\alpha = 0$ the unstable growth is predicted by Taylor's [2] result. It can be seen that as the rotation rate α increases, one of the $q = 1$ inertial wave solutions coalesces with the gravity wave solution. The critical rotation rate is predicted by (44) and is given by $\alpha_c = 0.49$. (c) $\mathscr{A} = \frac{1}{2}$ and $\delta = 4$. With the increase in δ we see an improvement between the full solution and Chandrasekhar's solution, giving better agreement than the low-rotation-rate asymptotics (32). (d) $\mathscr{A} = -\frac{1}{2}$ and $\delta = 4$. There is excellent agreement with Chandrasekhar's solution for $\alpha < 5$ compared with the low-rotation-rate asymptotics, but his solution remains in the unstable region as $\alpha \to \infty$, unlike the full solution. The critical rotation rate $\alpha_c = 7.78$ follows from (44). As in (b), one of the $q = 1$ inertial wave solutions coalesces with the gravity wave solution.

contain an infinite number of inertial waves corresponding to the higher values of q. Within this region the numerical contouring of $|\mathsf{M}| = 0$ fails and so the region has been grayed out.

In the stable cases $\mathscr{A} = \frac{1}{2}$, shown in Figs. 3(a) and 3(c), the effect of the rotation on the gravity wave on the interface is only to increase its frequency, hence the comments of Miles [13] indicating that the effects of rotation are not especially interesting for axisymmetric waves on a single layer of fluid. The asymptotic gravity wave solutions (32) are shown as the dashed lines extending away from the white circle on the vertical axes. They are shown dashed for $\alpha < 0.5$, after which we anticipate the approximations being less good, as the errors are $O(\alpha^2)$, and the solution is thereafter shown as dotted.

In the unstable cases $\mathscr{A} = -\frac{1}{2}$, shown in Figs. 3(b) and 3(d), the effect of rotation on the k_1 gravity wave at the interface is to change the sign of ω^2 from negative (unstable, a Rayleigh-Taylor instability) to positive (stable, standing-wave solutions). The rotation is able to completely stabilize the mode for $\alpha > \alpha_c$. It can be seen that as the rotation rate is increased the gravity wave solution coalesces with the dominant inertial wave solution. The predicted critical rotation rates are $\alpha_c \approx 0.49$ for $\delta = \frac{1}{4}$ and $\alpha_c \approx 7.78$ for $\delta = 4$. It can be seen that for moderate values of α there is significant improvement in the agreement between the numerical solution and Chandrasekhar's [16] solution for the larger value of δ, as expected (see Sec. II B 1). With the parameters used in Fig. 3(b), the asymptotic value of α_c calculated for large N is within 3.4% of that calculated using $N = 1$ modes, as in Eq. (44).

It can be shown that as a result of (41b), the key results of Sec. II B, (32) and (44), are independent of the $\Omega^2/(1 - \mu^2)$ term in Eq. (27), the only term that has an explicit dependence on the profile $z_0(r)$. As the low-rotation-rate approximation (32) and the critical rotation rate (44) are independent of this term, it follows that the unstable solution branch for ω can be well approximated by neglecting this term. Indeed, for low to moderate Atwood number ($\mathscr{A} \lesssim \frac{1}{2}$) then

$$\Phi \propto \int_0^a \left\{ \omega^2(\hat{\phi}_2 - \hat{\phi}_1)^2 - g\mathscr{A}\frac{\partial}{\partial z}(\hat{\phi}_2^2 - \hat{\phi}_1^2) \right\}\bigg|_{z=z_0(r)} r\,dr \tag{45}$$

is a reasonable approximation to (27), with approximate $O(\mathscr{A}^2)$ error. The calculated critical rotation rate for the example considered in Fig. 3(b) using (45), as opposed to (27), is $\alpha_c = 0.45$ compared to $\alpha_c = 0.49$, an error of approximately 7.8%.

C. Nonaxisymmetric instability $m \neq 0$

We now consider the more general case that includes nonaxisymmetric modes. Here the right-hand side of (29) can be nonzero and so $\omega \in \mathbb{C}$, giving the possibility of both growth and precession of the instability. As $\omega \in \mathbb{C}$ it follows that $k = k(\Omega, \omega) \in \mathbb{C}$ in general. The fact that k cannot be determined *a priori* for the whole solution space increases the difficulty of calculating solutions for the nonaxisymmetric cases compared to the axisymmetric cases.

1. Single-mode, low-rotation-rate, gravity wave solutions: Asymptotics

To find the corresponding low-rotation-rate asymptotics as in Sec. II B we expand both ω and k in terms of α. It follows from (29) for $\omega \sim \omega_0 + \omega_1\alpha^{1/2} + \omega_2\alpha + \cdots$ that

$$\frac{k}{k_0} \sim 1 + \frac{2m}{k_0^2 - m^2}\left(\frac{\alpha g}{a\omega_0^2}\right)^{1/2} - \frac{2m}{k_0^2 - m^2}\left[\left(\frac{a\omega_1^2}{g}\right)^{1/2} + \frac{m(k_0^2 + m^2)}{(k_0^2 - m^2)^2}\right]\left(\frac{\alpha g}{a\omega_0^2}\right) + O(\alpha^{3/2}), \tag{46}$$

where $k_0 \in \mathbb{R}$ satisfies

$$k_0\mathcal{J}_{m+1}(k_0) = m\mathcal{J}_m(k_0). \tag{47}$$

[Note that again there is a countable number of solutions k_{0n} but for clarity we will use the notation k_0 and understand that it may not be the first zero of (47).] Substituting in and following a similar

procedure to that in Sec. II B, the first two terms for ω satisfy

$$\frac{a\omega_0^2}{g} = \mathscr{A} k_0 \tanh(k_0\delta), \tag{48a}$$

$$\sqrt{\frac{a}{g}}\omega_1 = \frac{m}{k_0^2 - m^2}[1 + 2k_0\delta \operatorname{csch}(2k_0\delta)]. \tag{48b}$$

The leading-order term ω_0 is unchanged from (32), noting the change in definition of k_0. The ω_1 term is not present in Eq. (32), as a result of $m = 0$ in the axisymmetric case. However, we note that $\omega_1 \in \mathbb{R}$ and so this term can play no role in the growth or suppression of interfacial waves; it is merely contributing a modification to the precession velocity. We also note that ω_1 is independent of $\mathscr{A}$ and is therefore exactly the same as the first correction term found by Miles [see Eq. (5.5) in Ref. [14]].

For comparison with the second term on the right-hand side of (32) we now calculate $a(2\omega_0\omega_2 + \omega_1^2)/g$ and find it to be

$$2\left\{1 - \frac{2m^2 k_0^2}{\left(k_0^2 - m^2\right)^3} + 2k_0\delta \operatorname{csch}(2k_0\delta)\left[1 - \frac{m^2}{\left(k_0^2 - m^2\right)^2}\left(\frac{k_0^2 + m^2}{k_0^2 - m^2} + 2k_0\delta \coth(2k_0\delta)\right)\right]\right.$$
$$\left. - \frac{1}{8}k_0^2 \mathscr{A}^2 \operatorname{sech}(k_0\delta)^2\left[1 + \frac{4}{k_0^2 - m^2}\left(\frac{m^2}{k_0^2}\cosh(k_0\delta)^2 - k_0^2 G(m,k_0)\right)\right]\right\}, \tag{49}$$

where we use (41a)–(41c) and define

$$G(m,k) = \int_0^1 \frac{\mathcal{J}_m(kx)^2}{\mathcal{J}_m(k)^2}x^3 dx. \tag{50}$$

Provided k_0 is a solution of (47), then in the limit $m \to 0$, $G(m,k_0(m)) \to \frac{1}{6}$ and we may recover the axisymmetric $m = 0$ term in Eq. (32) from (49). The associated eigenvector with the solution described by (48) and (49) is

$$\boldsymbol{c} = \left(1, -1 - \frac{k_0}{2}\coth(k_0\delta)\left[1 + \frac{4}{k_0^2 - m^2}\left(\frac{m^2}{k_0^2} - k_0^2 G(m,k_0)\right)\right]\alpha + O(\alpha^2)\right) \tag{51}$$

and we note that therefore to leading order the solution in the lower layer is growing and precessing in the opposite direction to the fluid in the upper layer, as might have been anticipated.

It follows from (49) that $\omega_2 \in \mathbb{C}$ if $\omega_0 \in \mathbb{C}$ and so may contribute to both precession and growth–decay. Whether the growth rate of a wave mode is reduced or increased by a small amount of rotation, compared to its growth in a nonrotating system, is controlled by (49) too, since $\omega_1 \in \mathbb{R}$.

2. Single-mode, low-rotation-rate, inertial wave solutions: Asymptotics

As with the axisymmetric case, for ω^2 to have a leading-order contribution of $O(\alpha)$ we require (36) and hence (37) to be satisfied. Writing $\omega \sim \omega_1\alpha^{1/2} + \omega_2\alpha + \cdots$ and $k \sim k_0 + k_1\alpha^{1/2} + k_2\alpha + \cdots$ we have that

$$\frac{\omega_1^2 a}{g} = \frac{4}{1 + [2k_0\delta_q]^2} \quad \text{for} \quad \delta_q \equiv \frac{\delta}{q\pi}, \quad q \in \mathbb{N}. \tag{52}$$

The leading-order balance of (29) is therefore

$$\mathcal{J}_{m+1}(k_0) = \frac{m}{k_0}\left(1 + \frac{2}{\omega_1}\right)\mathcal{J}_m(k_0). \tag{53}$$

Combining (52) and (53), we have that for a given $m \neq 0$ and δ_q, k_0 must satisfy

$$1 + [2k_0\delta_q]^2 = \left(1 - \frac{k_0}{m}\frac{\mathcal{J}_{m+1}(k_0)}{\mathcal{J}_m(k_0)}\right)^2. \tag{54}$$

The solutions fall into two categories according to whether q is odd or even, as before. For q odd

$$\frac{\omega^2 a}{g} \sim \frac{4\alpha}{1 + [2k_0\delta_q]^2}\left\{1 \mp \frac{\alpha[2k_0\delta_q]^2}{2\delta}\{1 + 4[\delta_q^2 m^2 - G(m,k_0)]\}\right.$$

$$\times \left.\left[(1 + 4\delta_q^2 m^2)(1 + [2k_0\delta_q]^2) - \frac{8m\delta_q^2}{\omega_1}\right]^{-1}\right\}. \tag{55}$$

The expression for q even is lengthy and so here we note only the solutions for extreme values of δ. Specifically, if q is even and $m \neq 0$, then for $\delta \ll 1$,

$$\frac{\omega^2 a}{g} \sim 4\alpha\left\{1 \pm \frac{2\delta_q^2\alpha}{\delta}\{k_0^2[1 - 4G(m,k_0)] + 4m\} + O(\alpha^2)\right\}, \tag{56}$$

and for $\delta \gg 1$,

$$\frac{\omega^2 a}{g} \sim 4\alpha\left\{\frac{1}{[2k_0\delta_q]^2} \pm \frac{\alpha}{\delta}\frac{m}{\delta_q k_0^3} + O(\alpha^2)\right\}. \tag{57}$$

A further, higher-order, solution exists, provided $m \neq 0$, for $k \sim k_0 + O(\alpha)$, where $\mathcal{J}_m(k_0) = 0$ and

$$\frac{\omega^2 a}{g} \sim \left(\frac{2m}{k_0^2\delta}\right)^2\alpha^3\left\{1 - \frac{\alpha}{2\delta}\left[4G^+(m,k_0) - 1 + \frac{4}{k_0^2}\left(1 \pm \frac{2}{\mathscr{A}}\right)\right] + O(\alpha^2)\right\}, \tag{58}$$

where

$$G^+(m,k) = \int_0^1 \frac{\mathcal{J}_m^2(kx)}{\mathcal{J}_{m+1}^2(kx)}x^3 dx. \tag{59}$$

3. Single-mode critical rotation rate for stabilization

In Sec. II B 3 it was shown that for $\delta < \infty$ there exists a critical rotation rate Ω_c above which an axisymmetric wave mode can be stabilized for a given unstable Atwood number. Here we show that such a critical rotation rate does not exist in the case $m \neq 0$.

For $m \neq 0$ and $\Omega \sim \Omega_0[1 + (\Omega_1/\Omega_0)\omega + O(\omega^2)]$, (29) implies that

$$\frac{k}{k_0} \sim 1 - \frac{\omega}{2m\Omega_0} + O(\omega^2) \quad \text{where} \quad \mathcal{J}_m(k_0) = 0, \tag{60}$$

noting that $m \neq 0$ changes the definition of k_0 from the axisymmetric definition $\mathcal{J}_{m+1}(k_0) = 0$ to $\mathcal{J}_m(k_0) = 0$. The eigenvalue equation for Ω becomes

$$\frac{1 - \mathscr{A}^2}{\mathscr{A}^2}\left[a^2 m\Omega_0\mathcal{J}_{m+1}^2(k_0)\right]^2\omega^2 + O(\omega^3) = 0. \tag{61}$$

It can be seen that there is no nonzero critical rotation rate Ω_0 that can force the leading-order term in Eq. (61) to be zero. Therefore, unlike the axisymmetric $m = 0$ case, there does not exist a critical rotation rate that can be used to stabilize a given wave mode. However, a given wave mode may still be suppressed (or indeed excited) by rotation, but a change of stability cannot occur.
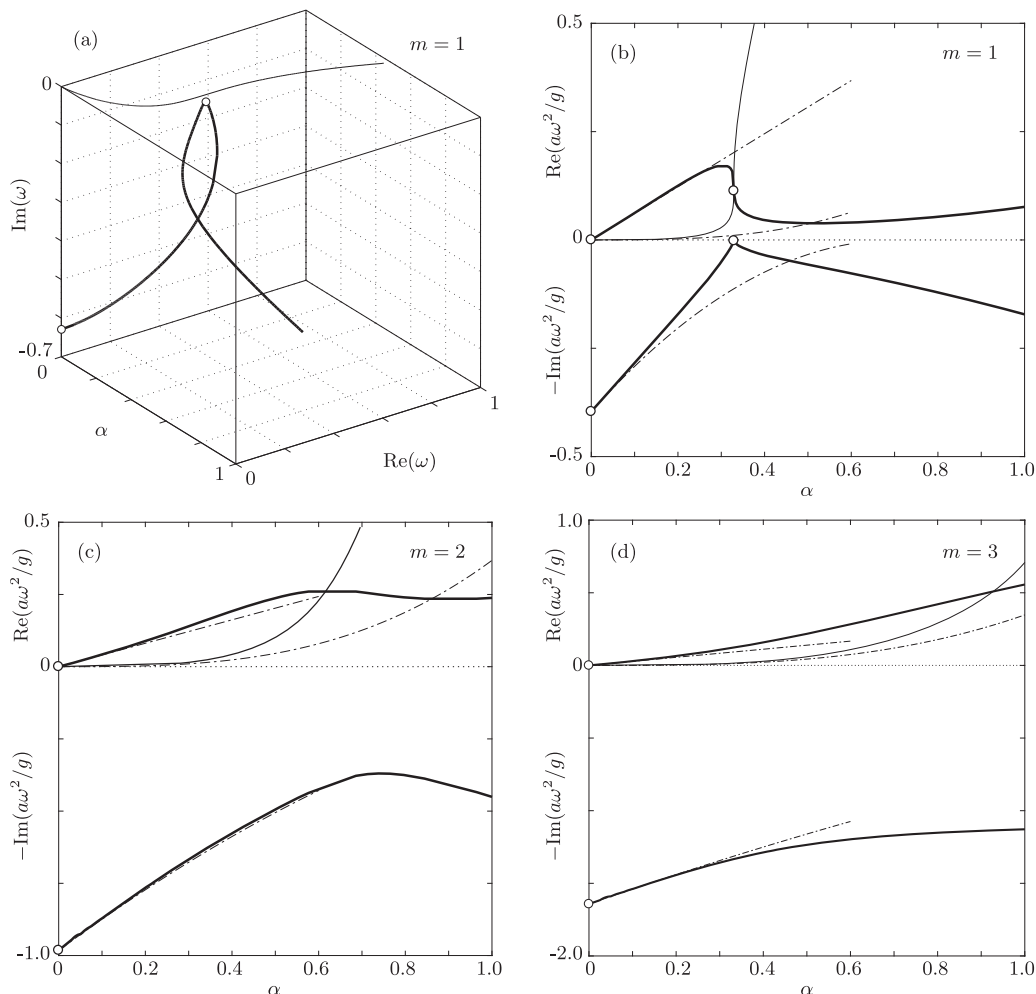
FIG. 4. (a) Constructed solution of $|\mathsf{M}| = 0$ for $\omega \in \mathbb{C}$ and $\mathscr{A} = -\frac{1}{2}$, $\delta = \frac{1}{4}$, $N = 1$, $n = 1$, and $m = 1$ (solid lines). (b)–(d) Projections of the solution squared, for comparison with Fig. 3(b). Bold solutions have nonzero imaginary component. It can be seen that unstable wave modes are not stabilized by increasing the rotation rate, but are suppressed initially. Asymptotic gravity wave approximations (48) and (49) to the solution are shown as dot-dashed lines. (Inertial wave solutions are not shown.)

4. Single-mode, arbitrary-rotation-rate solutions: Numerics

The solutions of the eigenvalue problem are calculated numerically for $N = 1$, $n = 1$, $\delta = \frac{1}{4}$, $\mathscr{A} = -\frac{1}{2}$, and $m = 1,2,3$ [see Fig. 3(b) for comparison with the axisymmetric case $m = 0$]. The numerical solution was calculated by evaluating the determinant of M for a given α over a plane $\omega \in \mathbb{C}$ (numerical integration was carried out using Simpson's rule). The zeros of the real part of $|\mathsf{M}|$ were contoured and intersections with the zero contour of the imaginary part of $|\mathsf{M}|$ were found. The solution was constructed by then allowing α to vary over the range $[0, \alpha_T]$ [see Fig. 4(a)]. Figures 4(b)–4(d) are projections of the three-dimensional solution to allow comparison with Fig. 3(b). The positive vertical axis shows a projection of $\mathrm{Re}(\omega)^2 a/g$ and the negative vertical axis shows a projection of $-\mathrm{Im}(\omega)^2 a/g$, so the plots coincide with the axisymmetric case when $\omega \in \mathbb{R}$ or $\omega \in \mathbb{R}$. It can be seen that for $m \neq 0$ the dominant gravity wave solution is not able to cross from
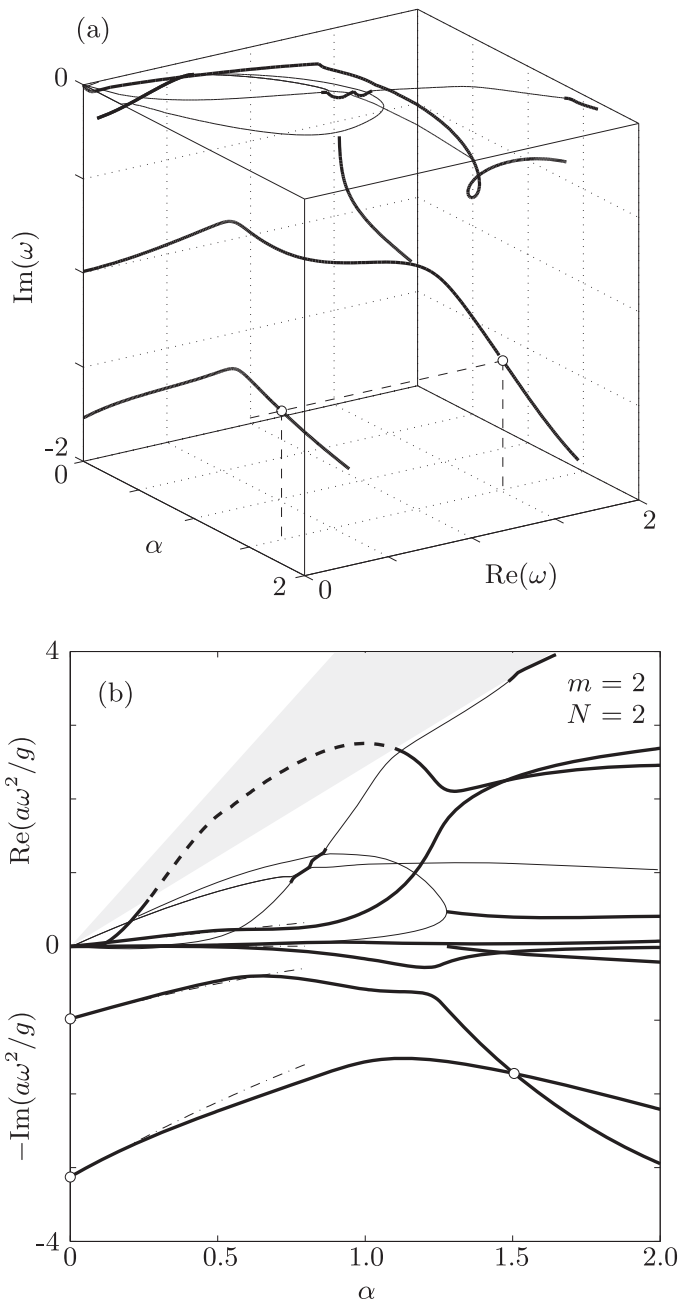
FIG. 5. Gravity wave solutions of $|\mathsf{M}| = 0$ for $\mathscr{A} = -\frac{1}{2}$, $\delta = \frac{1}{4}$, and $m = 2$ for $N = 2$ and $n = 1,2$, i.e., $k_{01} \approx 3.054$ and $k_{02} \approx 6.706$. Bold solutions have a nonzero imaginary component. (a) Three-dimensional representation of the solution: The most unstable branches cross at $\alpha \approx 1.505$, where $\omega_1 \approx 1.514i - 1.313i$ and $\omega_2 \approx 0.189i - 1.313i$, indicated by circles. (b) Projected solutions for comparison with Fig. 3(b). Although $\alpha_T = 1$, the α axis has been extended to show the possibility of rotation, causing some modes to become more unstable than others.

the unstable lower half of the domain into the stable upper half, unlike the $m = 0$ solution shown in Fig. 3(b).

5. Multiple-mode, arbitrary-rotation-rate solutions

Figure 5 shows the possible wave modes for $\mathscr{A} = -\frac{1}{2}$, $\delta = \frac{1}{4}$, $m = 2$, $N = 2$, and $n = 1, 2$. As the rotation rate is increased the unstable gravity wave modes are seen to be suppressed, though the suppression is greater for the more unstable $n = 2$ mode. The plot shows that suppressing a higher wave mode to such an extent that it becomes more stable than a lower wave mode is possible since the solution's projections cross [at $\alpha \approx 1.505$ and $\text{Im}(\omega) \approx -1.313$, shown as circles, though in this case the crossing occurs for $\alpha > \alpha_T$, where the solution is not strictly valid]. Comparing Fig. 4(c) with Fig. 5(b), it can be seen that the addition of a single extra mode significantly increases the number of possible modes of behavior.

D. Summary of key results

In Sec. II A the approach developed by Miles [14] to model surface waves on a rotating body of water was generalized to the two-layer case, allowing for either a stable (positive Atwood number) or an unstable (negative Atwood number) initial stratification. The dispersion relation for axisymmetric perturbations at low rotation rates was derived in Sec. II B, (32), which shows that gravitationally unstable perturbations may be made less unstable by rotating the system. This suggests that at least partial suppression of the Rayleigh-Taylor instability may be achieved through rotation of the system, though we note that the dispersion relation (32) is only valid in the low-rotation rate limit $a\Omega^2/g \ll 1$. In Sec. II B 3 an exact result (44) was found for the critical rotation rate required to completely stabilize an otherwise gravitationally unstable axisymmetric wave mode. This critical rotation rate depends on the aspect ratio of the system, which is the reason an exchange of stability was not found in the model of Chandrasekhar [16]. The critical rotation rate in Eq. (44) indicates that a rotation rate $\alpha_c = 12\delta$ is required to stabilize all axisymmetric wave modes, but the model solutions (28) are invalid for $\alpha > 4\delta$.

In Sec. II C the dispersion relation for asymmetric wave modes was derived (46)–(50). This dispersion relation includes axisymmetric perturbations $m = 0$ as a special case. In the asymmetric case $m \neq 0$ it was shown that the wave number cannot be determined *a priori*; it depends on both the rotation rate Ω and the mode frequency ω. The dispersion relation reveals, as might be anticipated, that the mode frequency contains both real and imaginary parts in general. Hence, the developing instability is characterized by both a growth and a precession of a given wave mode. It was also shown in Sec. II C 3 that a general critical rotation rate to stabilize an asymmetric mode does not exist, unlike the axisymmetric case.

III. DISCUSSION AND CONCLUSIONS

We have considered theoretically the effects of rotation upon the classical Rayleigh-Taylor instability. The dispersion relation for interfacial disturbances at low rotation rates (32) suggests that axisymmetric modes of a developing Rayleigh-Taylor instability may have their rate of growth inhibited by rotation. Indeed, if the critical rotation rate for the mode is below the threshold $2(gd)^{1/2}/a$, then (44) indicates that the mode may be stabilized indefinitely. Rotation was also seen in some cases to be able to slow the growth of asymmetric modes.

We can understand our observations in the following qualitative manner: A rotating fluid is known to organize itself into coherent vertical structures aligned with the axis of rotation, so-called Taylor columns [23], whereas a perturbation to an unstable two-layer density stratification will lead to baroclinic generation of vorticity at the interface, tending to break up any vertical structures. Hence the system under investigation undergoes competition between the stabilizing effect of the rotation, which is organizing the flow into vertical structures and preventing the two fluid layers passing each other, and the destabilizing effect of the denser fluid overlying the lighter fluid that generates

an overturning motion at the interface. With increased rotation rate the ability of the fluid layers to move radially, with opposite sense to each other, in order to rearrange themselves into a more stable configuration, is increasingly prohibited by the Taylor-Proudman theorem (see [24,25]). The radial movement is therefore reduced and the observed structures that materialize as the instability develops are smaller in scale.

[1] J. W. S. Rayleigh, Investigation of the character of the equilibrium of an incompressible heavy fluid of variable density, Proc. London Math. Soc. **s1-14**, 170 (1882).

[2] G. I. Taylor, The instability of fluid surfaces when accelerated in a direction perpendicular to their planes, I, Proc. R. Soc. London Ser. A **201**, 192 (1950).

[3] D. J. Lewis, The instability of fluid surfaces when accelerated in a direction perpendicular to their planes, II, Proc. R. Soc. London Ser. A **202**, 81 (1950).

[4] J. R. Freeman, M. J. Clauser, and S. L. Thompson, Rayleigh-Taylor instabilities in inertial confinement fusion targets, Nucl. Fusion **17**, 223 (1977).

[5] C.-Y. Wang and R. A. Chevalier, Instabilities in clumping and type Ia supernova remnants, Astrophys. J. **549**, 1119 (2001).

[6] D. Fultz, An experimental view of some atmospheric and oceanic behavioral problems, Trans. N.Y. Acad. Sci. **24**, 421 (1962).

[7] J. J. Tao, X. T. He, W. H. Ye, and F. H. Busse, Nonlinear Rayleigh-Taylor instability of rotating inviscid fluids, Phys. Rev. E **87**, 013001 (2013).

[8] J. Lindl, Development of the indirect-drive approach to inertial confinement fusion and the target physics basis for ignition and gain, Phys. Plasmas **2**, 3933 (1995).

[9] K. A. Baldwin, M. M. Scase, and R. J. A. Hill, The inhibition of the Rayleigh-Taylor instability by rotation, Sci. Rep. **5**, 11706 (2015).

[10] M. M. Scase and S. B. Dalziel, Internal wave fields and drag generated by a translating body in a stratified fluid, J. Fluid Mech. **498**, 289 (2004).

[11] M. M. Scase and S. B. Dalziel, Internal wave fields generated by a translating body in a stratified fluid: An experimental comparison, J. Fluid Mech. **564**, 305 (2006).

[12] M. M. Scase, K. A. Baldwin, and R. J. A. Hill, Magnetically induced rotating Rayleigh-Taylor instability [J. Vis. Expt. (to be published)].

[13] J. W. Miles, Free surface oscillations in a rotating fluid, Phys. Fluids **2**, 297 (1959).

[14] J. W. Miles, Free-surface oscillations in a slowly rotating fluid, J. Fluid Mech. **18**, 187 (1964).

[15] H. Lamb, *Hydrodynamics*, 6th ed. (Cambridge University Press, Cambridge, 1932).

[16] S. Chandrasekhar, *Hydrodynamic and Hydromagnetic Stability* (Dover, New York, 1961).

[17] H. Poincaré, Sur l'équilibre d'une masse fluide animée d'un mouvement de rotation, Acta Math. **7**, 259 (1885).

[18] R. W. Hart, Generalized scalar potentials for linearized three-dimensional flows with vorticity, Phys. Fluids **24**, 1418 (1981).

[19] M. J. Lighthill, *Waves in Fluids* (Cambridge University Press, Cambridge, 1978).

[20] B. A. Finlayson, *The Method of Weighted Residuals and Variational Principles* (Academic, New York, 1972).

[21] P. K. Sharma, R. P. Prajapati, and R. K. Chhajlani, Effect of surface tension and rotation on Rayleigh-Taylor instability of two superposed fluids with suspended particles, Acta Phys. Pol. A **118**, 576 (2010).

[22] G. F. Carnevale, P. Orlandi, and Y. Zhou, Rotational suppression of Rayleigh-Taylor instability, J. Fluid Mech. **457**, 181 (2002).

[23] G. I. Taylor, Experiments on the motion of solid bodies in rotating fluids, Proc. R. Soc. London Ser. A **104**, 213 (1923).

[24] J. Proudman, On the motion of solids in a fluid possessing vorticity, Proc. R. Soc. London Ser. A **92**, 408 (1916).

[25] G. I. Taylor, Motion of solids in fluids when the flow is not irrotational, Proc. R. Soc. London Ser. A **93**, 99 (1917).